DEVELOPMENT OF GD2 TARGETING THERANOSTICS FOR NEUROBLASTOMA

Sünnen, E.A.P.

ID: 5051819

Master Drug Innovation

Graduate School of Life Sciences

Utrecht University

Supervisors: Dr. Alex Poot

Dr. Berend van der Wildt

Major Research Project: 14th of January 2023 – 27th of October 2023

Collaboration between University Medical Center Utrecht and Princess Maxima Center

27th of October 2023

Abstract

Background – Dinutuximab-beta (Qarziba®), a monoclonal antibody targeting ganglioside GD2, has been approved for the treatment of high-risk neuroblastoma. Unfortunately, not all patients benefit from the treatment. This study will investigate the behavior of dinutuximab in more detail by radiolabelling dinutuximab.

Methods – By modification and labelling with Zirconium-89, the potentials of [^{89}Zr]Dinutuximab are explored by performing binding experiments using the free-antigen, high and low GD2 expressing cell lines, and tumor tissues.

Results – Radiolabelling resulted in a yield of 75%±8% (n=21) with a purity of >98% having an immune reactive fraction of 70%±5%. Significant results were found between high and low GD2 expressing cell lines ($p<0.0001$) but also when comparing to blocked conditions ($p<0.0001$). Tissue autoradiography was performed and differences between the treated and blocked conditions were observed ($p<0.0001$).

Conclusion – The first pre-clinical assessments on using radiolabelled dinutuximab resulted in consistent yield with high radiochemical purity. Whereafter binding of [^{89}Zr]Dinutuximab was demonstrated using the free-antigen, different cell lines, and tumor tissues.

Introduction

Neuroblastoma (NB), a heterogenous malignant neoplasm of the sympathetic nervous system is the most common extracranial solid tumor in children (1). They arise from the adrenal medulla or the paraspinal sympathetic ganglia of the neck, chest, abdomen, or pelvis, commonly presenting itself as a painless abdominal mass (1, 2). Although over time the prognosis after diagnosis is improved, it is still difficult to treat the patients presenting a metastatic, high-risk form of neuroblastoma (2).

Gangliosides are carbohydrates containing sphingolipids that have various subtypes that are widely expressed throughout the human body (3). In general, they have an important role in signal transduction as well as cell adhesion and recognition (4). They can be separated into a-series gangliosides which are generally expressed on normal tissues, and b-series gangliosides which are expressed during fetal development and are hardly present in adults. One subtype of these b-series gangliosides is disialoganglioside GD2, abundantly expressed on neuroectoderm-derived tumors, including NB, with minimal expression on peripheral nerve fibers and melanocytes (4-6). The ceramide tail of the ganglioside is embedded in the outer plasma membrane causing the sugar moiety, which derives from ceramides (4), to be exposed to the extracellular milieu (7).
As GD2 is highly expressed on the NB tumor tissue with limited expression on normal healthy tissue, it is a suitable target for immunotherapy (8). The human/mouse chimeric anti-GD2 antibody ch14.18 (dinutuximab-beta) has been developed to target the GD2 expressed on NB by triggering both complement-dependent cytotoxicity (CDC) and antigen-dependent cell-mediated cytotoxicity (ADCC) (9). It is approved in the European Union for the treatment of high-risk neuroblastoma (HR-NB) in patients > 12 months (4). The inclusion of immunotherapy in the treatment of HR-NB resulted in an increase in event free survival (63% vs. 44%) and overall survival (80% vs. 54%) at 5 years when comparing it to the standard, chemotherapy with isotretinoin (10-12). However, unfortunately one-third of the patients with HR-NB still relapses after treatment with anti-GD2 immunotherapy (9, 10). Besides that, treatment with dinutuximab is also associated with a lot of adverse events including neuropathic pain, peripheral neuropathy, hypersensitivity reactions and hypotension (4, 11). The most important side effect of treatment is neuropathic pain. The neuropathic pain that is induced in patients undergoing dinutuximab is mediated by the reactivity of the antibody with the GD2 expressed on the surface of nerve fibers. The mechanism of the neuropathic pain inducement is still unclear, but it is suggested that the same immune responses, the ADCC and CDC, contribute to the pain (4).

Theranostics, the use of closely related radiopharmaceuticals for diagnostic and therapeutic purposes, are currently very promising (13). Nowadays, the use of theranostics is implemented in the diagnosis and treatment of for example prostate cancer and neuroendocrine tumors by using Gallium-68 and Lutetium-177 (14, 15). Additionally, the use of theranostics for neuroblastoma is also not new. Iodine-123 and Iodine-131 can be coupled to meta-iodo-benzyl-guanidine (mIBG), a norepinephrine analog that accumulates in cells through the norepinephrine transporter (16, 17). However, treatment with mIBG has a response rate of 30% (17, 18), so there is still a lot of improvement possible for the treatment of HR-NB.

Immuno-Positron Emission Tomography (ImmunoPET) imaging using radiolabeled antibodies has progressed rapidly over the past decades (13, 19). Imaging with radiolabeled antibodies can serve as a potential biomarker to evaluate tumor targeting of antibodies (20). Zirconium-89 (^{89}Zr) is of great interest in the imaging field due to its fitting emission energy properties and half-life ($t_{1/2}$ = 78.4h), which often closely matches the circulation half-life of antibodies (19). Using a bifunctional chelator, possessing a reactive group for conjugation to free lysine and occasionally cystine residues on the antibody and a chelate for capturing of radioisotopes, ^{89}Zr can be coupled to an antibody (19). Successful modification and radiolabeling of antibodies has been described previously and many

clinical studies have been reported (13, 20). Despite the extensive research in adults, the use of immunoPET for pediatric cancers has barely been explored (13).

Combining this, the goal is to translate the knowledge of the use of immunoPET in adults to children and shine some light on the behavior of dinutuximab in the body to further investigate its potentials. This study will explore the first steps towards preclinical and clinical studies by investigating the binding of radiolabeled dinutuximab to tumor cells and tumor tissues.

Materials and methods

Antibody modification and labeling

Based on the protocol of Vosjan et al. (21) antibody modification and radiolabeling was set up. Dinutuximab-beta (Qarziba®) was obtained from the pharmacy of the Princess Maxima Center. The stock solution of dinutuximab (4.5mg/mL) was rebuffered in PBS using a PD10 SEC column, the pH was adjusted to 8.9-9.1 with 0.1M Na_2CO_3. *p*-Isothiocyanatobenzyl desferrioxamine (*p*-SCN-Bn-deferoxamine; abbreviated as DFO) was added in a 3:1 chelator antibody ratio, and after incubation for 30 minutes at 37 °C in the thermomixer at 300 RPM the reaction mixture was purified using a PD10 column to remove the unconjugated DFO.

[^{89}Zr]Zr-oxalic acid solution (Cyclotron B.V.) is neutralized using 2M Na_2CO_3 whereafter 0.5M HEPES buffer (pH = 6.8-7.2) was added to stabilize the pH. Modified dinutuximab was then added and the reaction mixture was incubated for 60 minutes at 37 °C in the thermomixer at 300 RPM. The mixture was purified using a PD10 column, all fractions were collected and the first analysis was done by measurement of individual fractions using a doses calibrator, to determine the radioactive yield.

Product quality assessment

For product quality assessment, instant Thin Layer Chromatography (iTLC) was performed using silica gel-coated paper strips as the stationary phase and a mobile phase of 0.01M EDTA in acetonitrile (50:50). The strips were analyzed using the phosphor imager (Amersham Typhoon; pixel size 100µm, sensitivity 4000V, laser 635nm), whereafter the iTLC strips were cut in the middle and measured in the γ-counter (Wizard; Open isotope spectrum measurement for 30 seconds) for the calculation of the purity. Purity was calculated as a percentage*:*

*(counts of bottom part / total counts of iTLC strip)*100%*

Additionally, Size Exclusion High-performance Liquid Chromatography (HPLC) was performed as a second method to determine the purity.

Lindmo immunoassay

Polysorp 96-wells plate strips were coated with the GD2 antigen, using a mixture of GD2 (500µg/mL), cholesterol (150µg/mL), and lecithin (250µg/mL) in absolute ethanol (1:1:1:47). 50µL of solution was added per well and evaporated in an oven for 1h at 45 °C. A negative control was created by coating the well strips with only cholesterol and lecithin. Excess antigen was removed by washing 3x with PBS whereafter the wells were blocked using 1% BSA in PBS. A dilution series of [^{89}Zr]Dinutuximab; 8µg/mL to 0.125µg/mL, was made and added to the wells. After overnight incubation at room temperature, the supernatant was collected and the wells were washed 3x with PBS. Hereafter the activity of the wells and supernatant was measured using the γ-counter. Immunoreactivity was calculated by:

(*counts well / (counts well + counts corresponding supernatant))*100%*

Cell binding experiments

Patient-derived tumoroids LVG and NB067 were selected based on GD2 expression that was determined using Fluorescence-activated Cell Sorting (FACS), expression data provided by Prof. Molenaar Princess Maxima Center (Figure 1). The LVG tumoroid has a high GD2 expression whereas NB067 has a rather low GD2 expression. The cells were cultured at 37 °C with 5% CO_2 using DMEM GlutaMAX supplemented with; Ham's F12 Nutrient mix, B-27 supplement (50X), N-2 supplement (100X), Penicillin-Streptomycin (10000U/mL), hEGF (500µg/mL), hFGF (500µg/mL), hIGF (200µg/mL), PDGF-AA (0.1mg/mL), and PDGF-BB (0.1mg/mL). Additionally, commercially available tumoroid KCNR was also obtained and is known to have a high GD2 expression. This line was cultured at 37 °C with 5% CO_2 in DMEM GlutaMAX containing the supplements; Fetal Bovine Serum (FBS), Penicillin-Streptomycin (10000U/mL), and Non-Essential Amino Acid (NEAA) (100X).

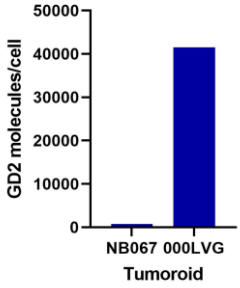

Figure 1: GD2 molecules per cell for the patient-derived tumoroids

Cells were removed from the culture flasks and put into a Falcon tube. The medium was refreshed and set to a volume of 10mL. The amount of cells was counted using trypan blue and Bio-Rad cell counter, and if necessary diluted to 4×10^6 cells/mL. To all, 1 mL of 10% BSA in PBS was added to obtain a final concentration of 1% BSA in the tubes to avoid stickiness. Two groups were then created; the treated and control group. The treated group received a 1:10 or 1:100 dilution of the [^{89}Zr]Dinutuximab (8µg/mL or 0.8µg/mL), whereas the control group received a 1:10 or 1:100 dilution of the [^{89}Zr]Dinutuximab together with 0.1mg of unlabeled dinutuximab. Cells were then incubated at room temperature on a roller band, keeping the tubes with cells in constant movement. Different incubation times were included; 15 minutes, 1 hour, 2 hours and 4 hours, whereafter the measurements took place. After centrifugation for 5 min at 300 RCF, the supernatant was collected and the cells were washed with 1% BSA in PBS by resuspending it and centrifuging it again 3 times. Hereafter the activity of the cell pellet as well as the supernatant was determined using the γ-counter. Binding percentage was calculated by:

(*counts cell pellet / (counts cell pellet + counts corresponding supernatant))*100%*

A negative control was implemented by performing this experiment with [^{89}Zr]-labeled IgG1 targeting Wall Teichoic Acids (WTA). To test if the on/off ratio of [^{89}Zr]Dinutuximab to GD2 will establish a new equilibrium, the KCNR and LVG cells were re-incubated after the measurements in 10mL of fresh medium together with 1mL of 10% BSA in PBS for 1h. The previously described protocol was then used to determine the new binding percentage.

Tissue autoradiography

Resected tumor tissues, 5 neuroblastoma tumors and a control tissue, were obtained from the Biobank of the Princess Maxima Center, prepared as 10µm coupes on glass slides and stored at -20 °C. After thawing, the tissues were rehydrated using 50mM TRIS-HCl buffer with 1% BSA (pH = 7.4). Once rehydrated, it was incubated for 1 hour with [^{89}Zr]Dinutuximab under three conditions. The treated group was given an incubation solution of 50mM TRIS-HCl buffer with 1% BSA, [^{89}Zr]Dinutuximab (0.05MBq/mL) and PBS, whereas the blocked group had an incubation solution of 50mM TRIS-HCl with

1% BSA containing [^{89}Zr]Dinutuximab (0.05MBq/mL) and unlabeled dinutuximab (2.25mg/mL) rebuffered in PBS. A control was implemented by blocking the tissues with an a-specific IgG1-antibody, Ipilimumab, used at 2.5mg/mL. This group received an incubation solution of 50mM TRIS-HCl buffer with 1% BSA, [^{89}Zr]Dinutuximab (0.05MBq/mL) and Ipilimumab in PBS. After incubation, the slides were washed twice in cold (5-7 °C) 5mM TRIS-HCl buffer (pH = 7.4, 1 minute) followed by a washing step with cold (5-7 °C) demineralized water (H_2O, 10 seconds). Once the slices were dry, they were put on a phosphor imaging plate for 1h and read by the phosphor imager.

Statistical Analyzes

All measurements were corrected for background activity. GraphPad Prism 9 was used for statistical analyzes and to create the corresponding figures. A 2-way ANOVA multiple comparisons test was used with a $p<0.05$ for significance. For the tissue autoradiography, analysis was performed using ImageJ software. Per tissue, three random areas (10mm^2) within the tissue were selected as Regions of Interest (ROIs) together with three random background ROIs to obtain grey values representing the tissue. These grey values were transformed into percentages, and these were analyzed using GraphPad Prism 9.

Results

In a miniaturized setting, 0.08mg of modified dinutuximab was labeled with 5-15MBq [^{89}Zr]Zr-oxalic acid in a total volume of 170µL. A radioactive yield of 75%±8% (n=21) was obtained with a purity of >98% after purification (Figure 2). HPLC analysis was performed but on both the Research HPLC as on the Quality Control (QC) HPLC. Abnormalities in the chromatograms were obtained in both machines. The Research HPLC presents an additional unexplainable radioactive peak at 10 minutes, whereas the QC-HPLC showed the correct product peak at 6.5 minutes but radioactive levels did not go down anymore, potentially due to sticking of the product in the radiation detector.

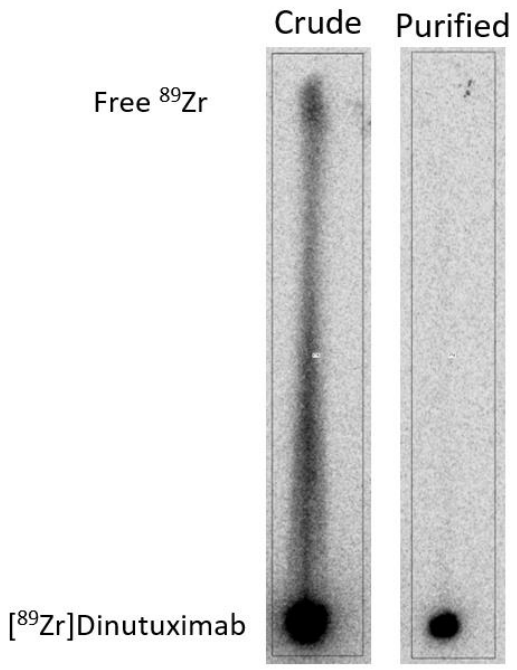

Figure 2: iTLC strips of [^{89}Zr]Dinutuximab crude reaction mixture and purified product

To test if the modified and radiolabeled dinutuximab is still functional, the Lindmo immuno-assay was performed. An immunoreactive fraction of 70%±5% was found with a negative control of 3%±1.5% (Figure 3), indicating that the antibody is still functional.

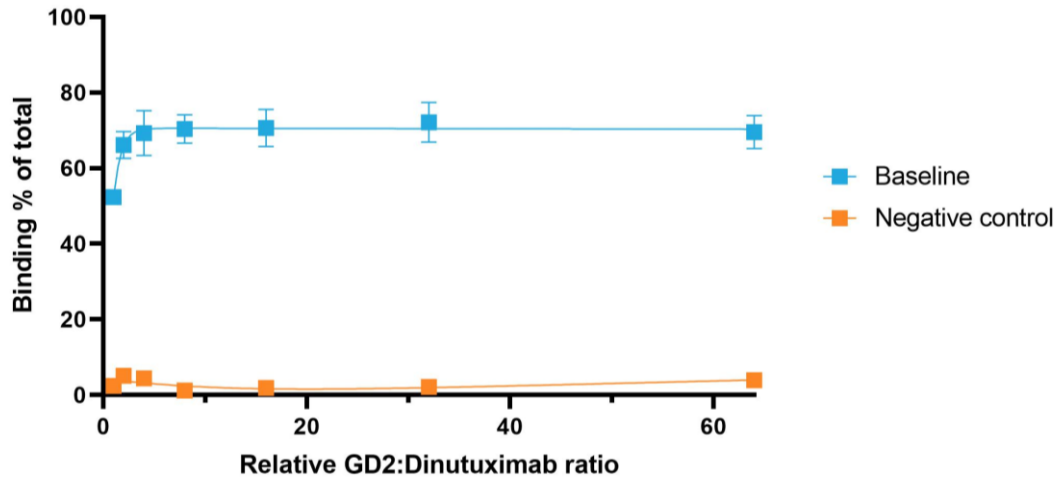

Figure 3: Lindmo immuno-assay

The [^{89}Zr]Dinutuximab was diluted 1:10 or 1:100 (8µg/mL or 0.8µg/mL) for the binding experiments, on one hand to make sure that there was enough activity left to distinguish it from the background, on the other hand to test if diluting would influence the binding. No differences were observed and therefore all the measurements were continued with a 1:10 dilution of the radiolabeled dinutuximab. Cell binding at the different incubation timepoints is visualized in Figure 4A. After an increase in binding from 15 min to 1h, longer incubation showed a decreasing binding trend for both the treated and the blocked group of all cell lines. The cell binding experiments presented the highest binding after 1h incubation, corresponding to a mean binding of 20.9% vs. 10.4% for the LVG treated vs. blocked, 4.4% vs. 2.5% for the NB cell line, and 20.6% vs. 8.7% for KCNR cells (Figure 4B). Significant differences were found between the treated and blocked group of the LVG and KCNR cell line, $p<0.0001$. Additionally, the comparison between the LVG and KCNR treated group to the NB treated group are found to be significant, $p<0.0001$. Indicating that the presented binding is actually binding of [^{89}Zr]Dinutuximab to GD2 on the cells. An IgG1-antibody targeting WTA was used as a negative control, where no binding was found. To see what the effect of the on/off ratio on the cells is and if a new equilibrium will be achieved, the cells were re-incubated with fresh medium after the first measurements. This test was only performed for the LVG and the KCNR cell line as the measurable activity for the NB cell line was too low to distinguish it from the background activity. Figure 4C presents the re-incubated binding percentages which, if summed up, correspond to a mean of 35.8%±2.7%. No differences between the cell lines or between blocked vs. treated were found to be significant.

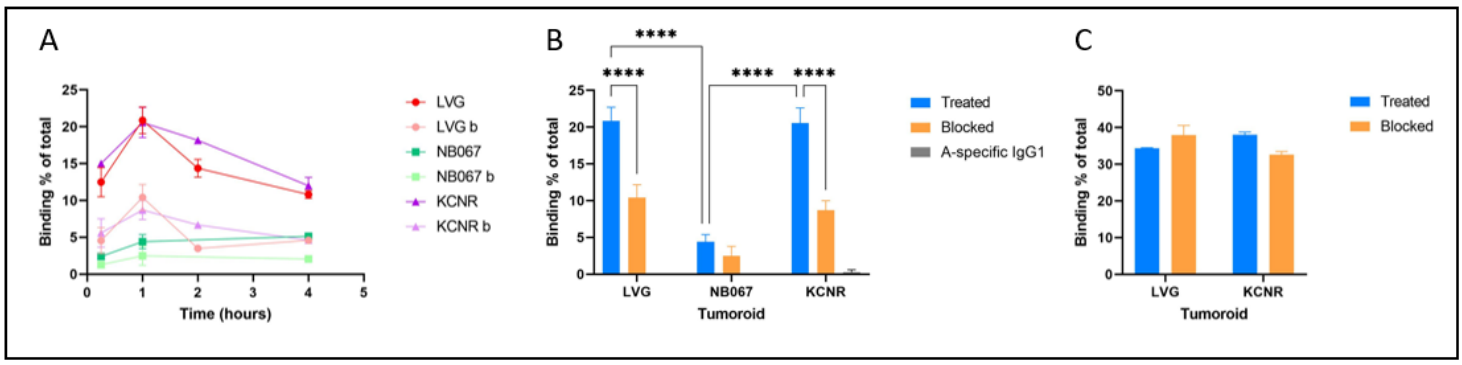

Figure 4: A) Cell binding of [^{89}Zr]Dinutuximab over time, 1h (B) and in re-incubated setting (C)

Figure 5A is the visualization of the 6 different tissues, 5 resected tumor tissues and a control tissue, incubated with [^{89}Zr]Dinutuximab. In all cases, the tissue of the treated group had higher grey values than the blocked group tissues and were all found to be significantly different $p<0.0001$ (Figure 5B). When comparing the treated group with the a-specifically blocked group, none was found to be significant (Figure 5C). The control tissue presented the lowest grey values in all groups, so the lowest binding of [^{89}Zr]Dinutuximab to GD2.

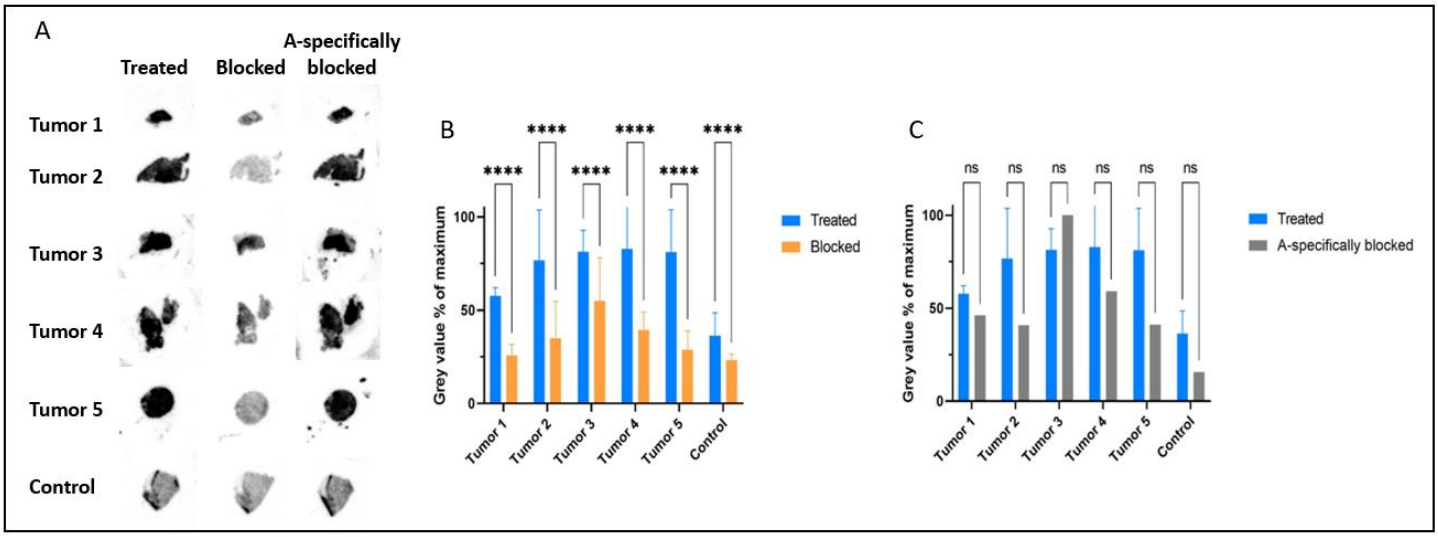

*Figure 5: A) Autoradiography of [^{89}Zr]Dinutuximab binding on 6 tissues. Tissue binding of treated vs. blocked group (B) and treated vs. a-specifically blocked group (C). **** = p<0.0001, ns = not significant*

Discussion

GD2 is one of the most prominent tumor-associated antigens and is highly expressed on neuroblastoma tumors (7). Targeting GD2 using dinutuximab improved the overall survival and event-free survival of patients with a high-risk form of neuroblastoma, but unfortunately not all patients benefit from the treatment (10, 11). By radiolabeling dinutuximab with ^{89}Zr, the behavior of dinutuximab in the body can be investigated in more detail and hopefully contribute to understanding why the treatment does not benefit all patients. This study focuses on the *in vitro* characteristics and abilities of [^{89}Zr]Dinutuximab as a first step towards pre-clinical and clinical use.

The two most important parameters for determining the functionality of radiolabeled antibodies are radiochemical purity and the immunoreactive fraction (22). The radiochemical purity is defined as the percentage of radionuclide which is bound to the antibody relative to all the activity in the product fraction. However, the chelator conjugation, radiolabeling technique, or storage conditions might affect the ability of the antibody to bind to the antigen. Therefore, the immune reactive fraction is determined to present the percentage of radiolabeled antibody that is able to bind to the antigen and is able to say something about the functional purity (22, 23). With a radiochemical purity after purification of >98% and an immunoreactive fraction of 70%±5%, it is assumed that the antibody presents itself as still functional with minimal a-specific binding (24). This was further explored in cell binding experiments in high and low GD2 expressing tumoroid models. By having significant differences between the high and low GD2 expressing cell lines, LVG and KCNR vs. NB, and significant blocking using unlabeled dinutuximab, it can be concluded that the binding found is of [^{89}Zr]Dinutuximab binding to GD2 (8).

Additionally, as a negative control, the experiment was performed with [^{89}Zr]-labeled IgG1 antibody targeting WTA, bacterial copolymers that are not present on neuroblastoma cells, 0% binding was found. During the re-incubated setting, the differences between treated and blocked were found not to be significantly different, this was expected due to the fact that the activity of the cell pellets of the

first measurements were considered 100%. By having a binding of 35.8%±2.7%, it presents that [^{89}Zr]Dinutuximab will establish a new equilibrium after re-incubation.
Incubation longer than 1h presented a decreasing trend in the binding of [^{89}Zr]Dinutuximab to GD2. Literature suggests that cells are able to respond to physical changes in their microenvironment (25). By having the cells in constant movement in a closed-off environment at room temperature, it can influence the cells and even induce cell death. To confirm that the reduced binding of [^{89}Zr]Dinutuximab to neuroblastoma cells at time points beyond 1h is due to cell death, a cell viability test could be performed to investigate the effect of these conditions for a longer period of time. Besides that, GD2 is also known to shed from neuroblastoma cells (26, 27) which might be induced by the constant movement. Therefore, the amount of GD2 present on the cells could be lower than the actual GD2 present and can lower the found binding.
Apart from cell binding and blocking assays, in vitro autoradiography can be used to assess the affinity and binding selectivity of an antibody to its target expressed on tissues (28, 29). The use of tissue autoradiography is argued to present the most closely approximate of characteristics that the tracer would present in living tissues (28).
The tissues for this study are resected material, after a round of chemo during surgery and fresh frozen, so representing the tumor condition when [^{89}Zr]Dinutuximab would be included in the treatment. Besides that, a lot about the tissues is unknown. Hematoxylin and eosin (H&E) staining of the slides was performed by the Biobank of the Princes Maxima Center but could not be analyzed yet. So it is still unclear how the tumor cells, and thus the GD2 expression, are distributed within the tissues. Regardless of the lack of information about the tissues, binding of [^{89}Zr]Dinutuximab to GD2 on these tissues is demonstrated. By blocking with unlabeled dinutuximab there is a significantly lower binding, and when blocked with an a-specific IgG1-antibody there is no difference in binding found with the treated group. So, when the analysis of the H&E stained slides is performed the relation between the distribution of GD2 throughout the tissues and the found binding can be investigated in more detail.

Conclusion and future prospects

The focus of this study was to take the first steps towards pre-clinical and clinical use of radiolabelled dinutuximab. Labelling dinutuximab with ^{89}Zr resulted in consistent yield with high radiochemical purity of >98%. Specific binding of [^{89}Zr]Dinutuximab to GD2 was demonstrated using the free antigen, cells with high and low GD2 expression and tumor tissues. The next step will be to perform *in vivo* imaging studies in tumor bearing mice to investigate the tumor uptake and biodistribution of [^{89}Zr]Dinutuximab.

Additionally to labelling dinutuximab with ^{89}Zr, the first steps in optimization of labelling dinutuximab with therapeutic isotopes Lutetium-177 and Actinium-225 were made to increase the radioactive yield and achieve consistency of the labelling. This process will be followed by performing radio-immunoassay and cell viability assays to explore the potential benefits of using therapeutically radiolabelled dinutuximab.

Overall, the first pre-clinical assessments on using radiolabelled dinutuximab showed promising results. By exploring further *in vivo*, hopefully the translation into the clinic can be made and [^{89}Zr]Dinutuximab can serve as a prognostic factor in the treatment plan of HR-NB.

References

1. Park JR, Eggert A, Caron H. Neuroblastoma: biology, prognosis, and treatment. Pediatr Clin North Am. 2008;55(1):97-120, x.
2. Newman EA, Abdessalam S, Aldrink JH, Austin M, Heaton TE, Bruny J, et al. Update on neuroblastoma. Journal of pediatric surgery. 2019;54(3):383-9.
3. Nazha B, Inal C, Owonikoko TK. Disialoganglioside GD2 Expression in Solid Tumors and Role as a Target for Cancer Therapy. Frontiers in Oncology. 2020;10.
4. Mastrangelo S, Rivetti S, Triarico S, Romano A, Attinà G, Maurizi P, et al. Mechanisms, characteristics, and treatment of neuropathic pain and peripheral neuropathy associated with dinutuximab in neuroblastoma patients. International Journal of Molecular Sciences. 2021;22(23):12648.
5. Ladenstein R, Pötschger U, Valteau-Couanet D, Luksch R, Castel V, Ash S, et al. Investigation of the role of dinutuximab beta-based immunotherapy in the SIOPEN high-risk neuroblastoma 1 trial (HR-NBL1). Cancers. 2020;12(2):309.
6. Voeller J, Sondel PM. Advances in anti-GD2 immunotherapy for treatment of high-risk neuroblastoma. Journal of pediatric hematology/oncology. 2019;41(3):163.
7. Horwacik I, Golik P, Grudnik P, Kolinski M, Zdzalik M, Rokita H, et al. Structural Basis of GD2 Ganglioside and Mimetic Peptide Recognition by 14G2a Antibody. Mol Cell Proteomics. 2015;14(10):2577-90.
8. Schmitt J, Schwenck J, Maurer A, Przybille M, Sonanini D, Reischl G, et al. Translational immunoPET imaging using a radiolabeled GD2-specific antibody in neuroblastoma. Theranostics. 2022;12(13):5615.
9. Terzic T, Cordeau M, Herblot S, Teira P, Cournoyer S, Beaunoyer M, et al. Expression of Disialoganglioside (GD2) in Neuroblastic Tumors: A Prognostic Value for Patients Treated With Anti-GD2 Immunotherapy. Pediatr Dev Pathol. 2018;21(4):355-62.
10. Yu AL, Gilman AL, Ozkaynak MF, London WB, Kreissman SG, Chen HX, et al. Anti-GD2 antibody with GM-CSF, interleukin-2, and isotretinoin for neuroblastoma. New England Journal of Medicine. 2010;363(14):1324-34.
11. Wahba A, Wolters R, Foster JH. Neuroblastoma in the Era of Precision Medicine: A Clinical Review. Cancers. 2023;15(19):4722.
12. Yu AL, Gilman AL, Ozkaynak MF, Naranjo A, Diccianni MB, Gan J, et al. Long-Term Follow-up of a Phase III Study of ch14.18 (Dinutuximab) + Cytokine Immunotherapy in Children with High-Risk Neuroblastoma: COG Study ANBL0032. Clin Cancer Res. 2021;27(8):2179-89.
13. Poot AJ, Lam MGEH, van Noesel MM. The Current Status and Future Potential of Theranostics to Diagnose and Treat Childhood Cancer. Frontiers in Oncology. 2020;10.
14. van der Sar ECA, de Keizer B, Lavalaye J, de Klerk JMH, van Golen LW, Vogel WV, et al. Lutetium-177 PSMA for prostate cancer, current developments and challenges. TvNG. 2023;2023-02.
15. Banerjee SR, Pomper MG. Clinical applications of Gallium-68. Applied Radiation and Isotopes. 2013;76:2-13.
16. Chung HW, Park JW, Lee EJ, Jung KH, Paik JY, Lee KH. 131I-MIBG targeting of neuroblastoma cells is acutely enhanced by KCl stimulation through the calcium/calmodulin-dependent kinase pathway. Cancer Biother Radiopharm. 2013;28(6):488-93.
17. Rubio PM, Galán V, Rodado S, Plaza D, Martínez L. MIBG Therapy for Neuroblastoma: Precision Achieved With Dosimetry, and Concern for False Responders. Front Med (Lausanne). 2020;7:173.
18. Wilson JS, Gains JE, Moroz V, Wheatley K, Gaze MN. A systematic review of 131I-meta iodobenzylguanidine molecular radiotherapy for neuroblastoma. European journal of cancer. 2014;50(4):801-15.
19. Wei W, Rosenkrans ZT, Liu J, Huang G, Luo Q-Y, Cai W. ImmunoPET: Concept, Design, and Applications. Chemical Reviews. 2020;120(8):3787-851.

20. Jauw YWS, Menke-van der Houven van Oordt CW, Hoekstra OS, Hendrikse NH, Vugts DJ, Zijlstra JM, et al. Immuno-Positron Emission Tomography with Zirconium-89-Labeled Monoclonal Antibodies in Oncology: What Can We Learn from Initial Clinical Trials? Frontiers in Pharmacology. 2016;7.
21. Vosjan MJ, Perk LR, Visser GW, Budde M, Jurek P, Kiefer GE, et al. Conjugation and radiolabeling of monoclonal antibodies with zirconium-89 for PET imaging using the bifunctional chelate p-isothiocyanatobenzyl-desferrioxamine. Nat Protoc. 2010;5(4):739-43.
22. Konishi S, Hamacher K, Vallabhajosula S, Kothari P, Bastidas D, Bander N, et al. Determination of immunoreactive fraction of radiolabeled monoclonal antibodies: what is an appropriate method? Cancer biotherapy & radiopharmaceuticals. 2004;19(6):706-15.
23. Lindmo T, Boven E, Cuttitta F, Fedorko J, Bunn Jr P. Determination of the immunoreactive function of radiolabeled monoclonal antibodies by linear extrapolation to binding at infinite antigen excess. Journal of immunological methods. 1984;72(1):77-89.
24. Voss SD, Smith SV, DiBartolo N, McIntosh LJ, Cyr EM, Bonab AA, et al. Positron emission tomography (PET) imaging of neuroblastoma and melanoma with 64Cu-SarAr immunoconjugates. Proceedings of the National Academy of Sciences. 2007;104(44):17489-93.
25. Petzold J, Gentleman E. Intrinsic mechanical cues and their impact on stem cells and embryogenesis. Frontiers in cell and developmental biology. 2021;9:761871.
26. Balis FM, McCully CL, Busch CM, Fox E, Warren KE. Pharmacokinetics of the disialoganglioside, G(D2), a circulating tumor biomarker for neuroblastoma, in nonhuman primates. J Circ Biomark. 2021;10:26-9.
27. Kholodenko IV, Kalinovsky DV, Doronin II, Deyev SM, Kholodenko RV. Neuroblastoma Origin and Therapeutic Targets for Immunotherapy. Journal of Immunology Research. 2018;2018:7394268.
28. IAEA. Guidance for preclinical studies with radiopharmaceuticals. IAEA RADIOISOTOPES AND RADIOPHARMACEUTICALS SERIES No 8 2021.
29. Griem-Krey N, Klein AB, Herth M, Wellendorph P. Autoradiography as a simple and powerful method for visualization and characterization of pharmacological targets. JoVE (Journal of Visualized Experiments). 2019(145):e58879.